

We are IntechOpen, the world's leading publisher of Open Access books Built by scientists, for scientists

6,900

Open access books available

185,000

International authors and editors

200M

Downloads

Our authors are among the

154

Countries delivered to

TOP 1%

most cited scientists

12.2%

Contributors from top 500 universities



WEB OF SCIENCE™

Selection of our books indexed in the Book Citation Index
in Web of Science™ Core Collection (BKCI)

Interested in publishing with us?
Contact book.department@intechopen.com

Numbers displayed above are based on latest data collected.
For more information visit www.intechopen.com



Mechanism of Photoluminescence in Erbium-Doped Chalcogenide

Volodymyr V. Halyan and Inna A. Ivashchenko

Abstract

The monograph describes the technique of the synthesis of glasses and the method of the growth of erbium-doped single crystals. The photoluminescence spectra of $\text{Ag}_{0.05}\text{Ga}_{0.05}\text{Ge}_{0.95}\text{S}_2\text{-Er}_2\text{S}_3$ glasses and glasses from the $\text{Ga}_2\text{S}_3\text{-La}_2\text{S}_3\text{-Er}_2\text{S}_3$ system have been investigated in the visible and near-infrared ranges. According to the energy transitions in the erbium ions, a radiation mechanism for conversion and up-conversion luminescence has been established. The role of structural ordering and the influence of defects on the radiation efficiency of Er^{3+} ions have been investigated. The spectra of photoluminescence of $(\text{Ga}_{54.59}\text{In}_{44.66}\text{Er}_{0.75})_2\text{S}_{300}$ and $(\text{Ga}_{69.75}\text{La}_{29.75}\text{Er}_{0.5})_2\text{S}_{300}$ single crystals have been studied. The efficiency of the radiation of the amorphous and crystalline materials has been compared. Also, the temperature dependence of the integral intensity of the radiation of glasses and single crystals has been studied. It is established that in a limited temperature range, these materials can be used for the manufacture of non-contact optical thermosensors.

Keywords: glass, single crystal, photoluminescence, energy transition, radiation mechanism, visible, and near-infrared ranges

1. Introduction

Modern scientific and technological progress requires the constant search for and introduction of new multifunctional materials. One of the directions in the search for new semiconductor materials is the study of multicomponent systems of binary and ternary phases, which are promising for practical use. This is due to increasing requirements for semiconductor materials in connection with the development of new or modernization of known technical devices. To expand the list of materials, a study of chalcogenide quasi-ternary systems was undertaken.

Chalcogenide semiconductor materials were the object of research for many decades. The best studied glassy and crystalline chalcogenides are based on the Ge-X , Ga-X , As-X systems ($\text{X} = \text{S}, \text{Se}, \text{Te}$) modified by the admixture of Hg , Sb , Pb , Ag , etc. [1–3]. An important feature of chalcogenide glass is that the introduced admixtures are electrically and optically inactive. As a rule, they do not create localized states in the band gap. When introduced into a glass-forming matrix, admixture atoms rebuild their local environment resulting in the saturation of their valence bonds. Exceptions are the admixtures of bismuth, platinum, and gold into arsenic sulfide [4–6].

Special attention is devoted to the research of the luminescence properties of chalcogenide crystals and glasses due to practical application in optoelectronic technology. Their unique properties create advantages over other light-emitting materials and cause considerable interest both from the fundamental and the applied point of view. The chalcogenide materials combine high transparency in the visible, near-infrared, and medium-infrared spectral regions. By selecting the optimal component composition, it is possible to obtain wide areas of glass formation and to introduce relatively high concentration of rare earth metals (RE). Additionally, chalcogenides are characterized by high refractive index, good nonlinear optical properties, resistance to aggressive media, and easy manufacture technology. The addition of RE (Er, La, Eu, Pr, Tb, Ho, etc.) to the crystalline or amorphous chalcogenide medium creates potential opportunities for their use as high-quantum output luminophores, optical filters, active media in laser technology, in telecommunication devices, as well as non-contact optical temperature, and γ -irradiation sensors. The chalcogenide media that are activated by RE ions can also exhibit both conversion and up-conversion photoluminescence (PL) which creates the prerequisites for the design of effective converters from the infrared range to visible light.

Therefore, the preparation of chalcogenide glasses and crystals doped with rare earths and the study of their emission properties under different temperature and irradiation regimes are an extremely important area of modern solid-state physics and chemistry.

2. Synthesis of glasses and single crystal growth

Elementary high-purity substances were used for the synthesis of samples: Ag (99.99 wt.% of the principal), Ga, In, Ge (99.999 wt.% purity), La, Er (99.9 wt.%), and S, Se (99.997 wt.%). The elements for single crystal growth were further purified by double vacuum distillation. The weight of the starting components for the glasses was 3 g; the batches for the synthesis of single crystals were 10 g.

The samples were synthesized in cylindrical quartz containers with 9–15 mm diameter. The loaded ampoules were evacuated to a residual pressure of 1.33×10^{-2} Pa. The synthesis of glasses was performed in a shaft-type furnace with a temperature control system of ± 5 K accuracy.

The alloys for the glasses of the $\text{La}_2\text{S}_3\text{-Er}_2\text{S}_3\text{-Ga}_2\text{S}_3$ system with sample weight 2 g were pre-synthesized at 870 K and 24 h exposure. Obtained samples were ground in an agate mortar and loaded into quartz containers with a spherical bottom of 1 cm diameter. The heating was stepwise, first to 1070 K at a rate of 50 K/h and then to 1420 K at a rate of 40 K/h. After 3 h exposure at the maximum temperature, the samples were quenched into saturated NaCl solution with crushed ice.

Synthesis of the $\text{Ag}_{0.05}\text{Ga}_{0.05}\text{Ge}_{0.95}\text{S}_2\text{-Er}_2\text{S}_3$ glass alloys was performed in two stages. Initially, the ampoules were heated in the flame of an oxygen-gas burner to complete bonding of elemental sulfur. Then the ampoules were placed in a shaft-type furnace and heated at a rate of 20 K/h to 1273 K. The samples were kept at the maximum temperature for 10 h with periodic vibration. The alloys were cooled at a rate of 10–20 K/h to annealing temperature. The homogenizing annealing was held for 500 h at 720 K. The annealed alloys were quenched into 25% aqueous NaCl solution at room temperature.

To prevent the spatter of melt during quenching as well as to reduce losses due to the vapor phase condensing on the walls of the container, the special form of the container was used (**Figure 1**), and the upper part was thermostated by asbestos cord after the binding of sulfur in the oxygen-gas burner flame was used.

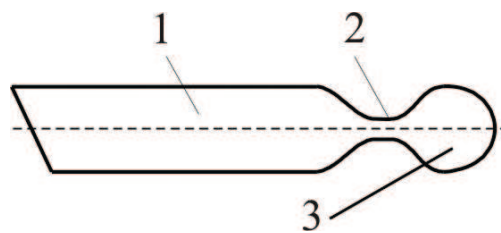


Figure 1.
Container for the synthesis of glassy alloys: (1) cylindrical part of the container; (2) neck; (3) thin-walled pear-shaped chamber.

The method and conditions for the single crystal growth of the phases $(\text{Ga}_{55}\text{In}_{45})_2\text{S}_{300}$ and $(\text{Ga}_{55}\text{In}_{45})_2\text{S}_{300}:0.3 \text{ at. \% Er}$ [7] were selected from the $\text{Ga}_2\text{S}_3\text{-In}_2\text{S}_3$ phase diagram; the supercooling temperature was determined from the cooling curves of the sample thermograms. The solution-melt method was used; supercooling of the solution melt was 70 K. The synthesis of the initial alloys at the maximum temperature of 1200 K and the growth of crystals were combined in evacuated graphitized quartz container with a conical bottom and a 2 mm diameter neck. The growth process was performed in a vertical two-zone furnace. The maximum temperature was 1200 K; the temperature gradient at the solid-melt interface was 20 K/cm. After melting the batch, the ampoule was lowered at the maximum rate. After crystallization of 10 mm of melt along the length of the ampoule, the growth was stopped, followed by re-melting of 6.0–8.0 mm of the crystallized portion and by annealing the seed during 100 h. Further growth of the single crystal was performed at a rate of 5 mm/day. After completion of the process, both furnaces were cooled to 820 K at a rate of 50–70 K/day, and the resulting single crystal

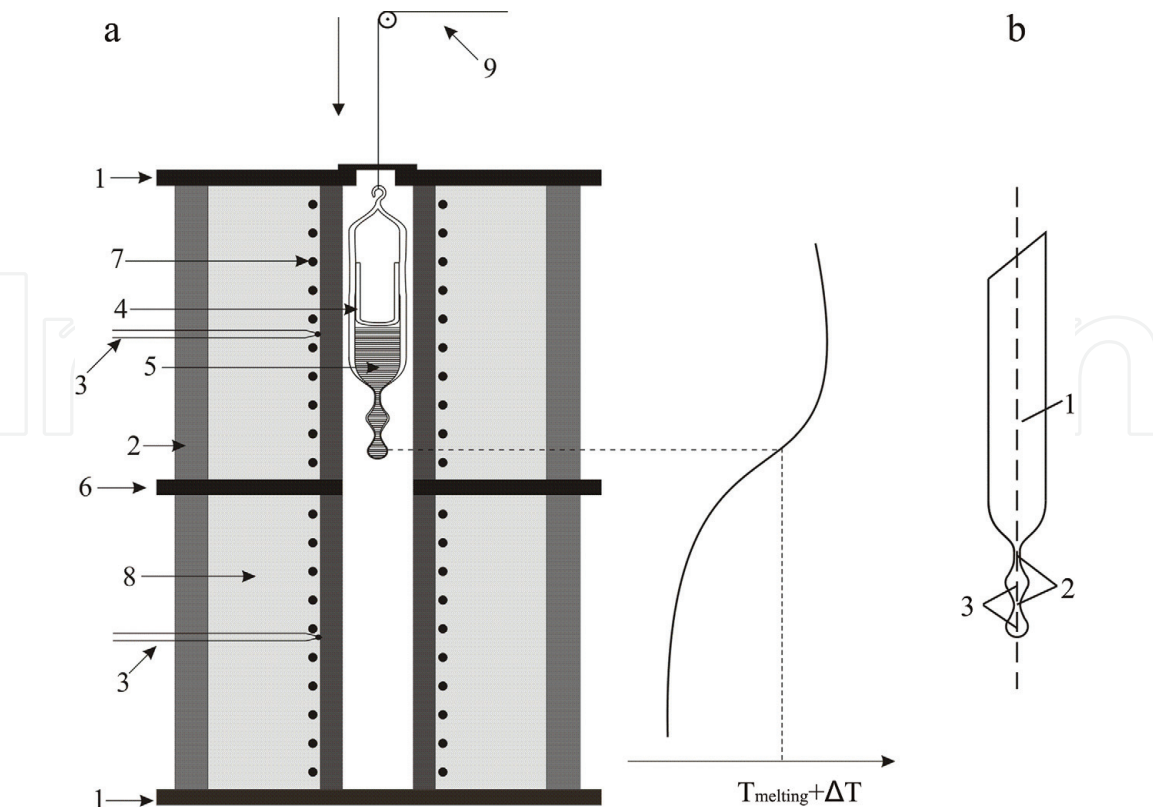


Figure 2.
Growth unit setup and the container for the single crystal growth: (a) 1—metal flange, 2—asbestos-cement casing, 3—Pt/Pt-Rh-thermocouple, 4—growth container, 5—melt, 6—metal disk, 7—heater, 8—thermal insulator, and 9—pulley for moving ampoules; (b) 1—cylindrical part of the container, 2—necks for seed formation, and 3—pear-shaped chambers.

was annealed for 100 h. After that, the furnace was switched off. The single crystals of orange color, 14 mm in diameter and 20 mm in length, were obtained.

The single crystal growth was performed in a setup installation shown in **Figure 2a** along with the temperature distribution along the heaters. The temperature in the growth zone was maintained by precision temperature controllers with an accuracy of ± 0.5 K.

A version of a container with two pear-shaped chambers connected by a neck was used for the growth of single crystals (**Figure 2b**). This increases the probability of obtaining a single crystal with its subsequent growth to a larger size in the cylindrical portion of the container.

Independent temperature control in different areas of the heater allows us to vary the gradient at the solid-melt interface within 3–5 K/mm. The growth rate was within 2 mm/day. The vertical movement of the plane of the crystallization zone was ensured by moving the container while the heater was at a fixed position.

3. Photoluminescence in chalcogenide glasses

An analysis of literature sources shows that chalcogenide glasses, unless doped with REs, do not usually exhibit luminescent properties at room temperature. For a long time, this limited their use in optoelectronic technology. Investigations of RE-free glasses with the substitution of selenium for sulfur revealed the existence of a broad unstructured PL band at 80 K (**Figure 3**).

The glasses of the $\text{AgGaSe}_2 + \text{GeS}_2 \rightleftharpoons \text{AgGaS}_2 + \text{GeSe}_2$ system excited by a laser with 532-nm wavelength exhibit at low-temperature luminescence with a single maximum in the near-infrared range ($\lambda_m \approx 1150\text{--}1180$ nm) with an emission band half-width $\Delta E \approx 0.26\text{--}0.30$ eV (**Figure 3a**), which is typical of the recombination luminescence in disordered systems. The intensity of the luminescence maximum depends on the content of Se (when sulfur is substituted with selenium, **Figure 3b**). The dependence is complex and to a large extent is due to the change in the level of luminescence excitation (caused by the shift of the absorption edge with increasing concentration of selenium in the alloy [8]). An important feature of the luminescence spectrum is that the position of the luminescence maximum is close to the center of the band gap (as determined by the position of optical absorption edge [8]). This is well illustrated by the model of Mott and Davis [9] stating that a band of localized states (several tenths of eV wide) is located in the center of the band

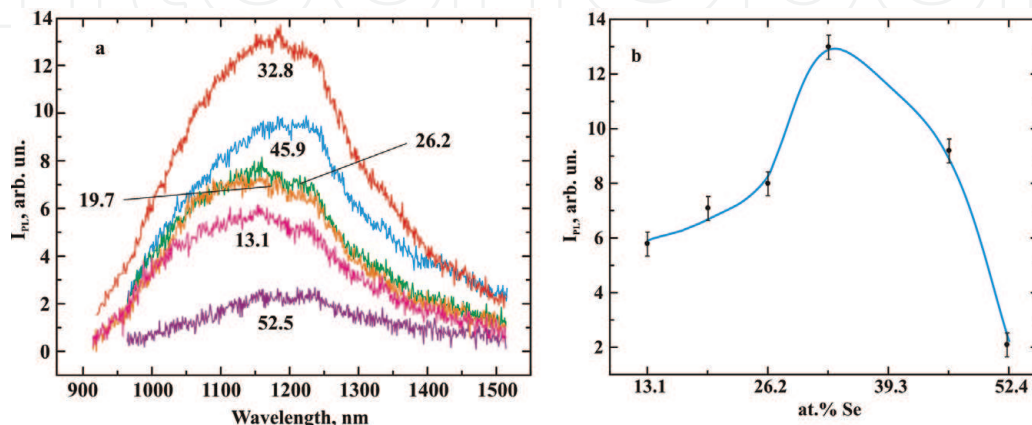


Figure 3.

(a) Luminescence spectra of the glassy alloys of the $\text{AgGaSe}_2 + \text{GeS}_2 \rightleftharpoons \text{AgGaS}_2 + \text{GeSe}_2$ system (at.% Se is indicated). (b) Dependence of the emission intensity at the maximum ($\lambda_m \approx 1180$ nm) on the content of Se (excitation wavelength 532 nm, temperature 80 K).

gap of chalcogenide glass semiconductors. Optical transitions of electrons into this band can cause luminescence with the energy of light quanta close to the half-width of the band gap.

The glassy alloy $\text{Ag}_{0.05}\text{Ga}_{0.05}\text{Ge}_{0.95}\text{S}_2$ is characterized by the largest transparency window [8] among other glasses of the $\text{AgGaSe}_2 + \text{GeS}_2 \rightleftharpoons \text{AgGaS}_2 + \text{GeSe}_2$ system. This alloy was doped with an Er_2S_3 admixture. PL spectra investigation (**Figure 4**) was performed on the glasses $(100 - X)\text{Ag}_{0.05}\text{Ga}_{0.05}\text{Ge}_{0.95}\text{S}_2 - (X) \text{Er}_2\text{S}_3$, where $X = 0.42, 0.25$, and $0.18 \text{ mol.}\%$ ($0.27, 0.16$, and $0.12 \text{ at.}\%$ Er, respectively).

The excitation was performed by a laser with 980-nm wavelength which corresponds to the $^4\text{I}_{15/2} \rightarrow ^4\text{I}_{11/2}$ transition, whereas the PL emission band is due to the $^4\text{I}_{13/2} \rightarrow ^4\text{I}_{15/2}$ transition in Er^{3+} ion, respectively. The PL intensity increases with Er content. The position of the luminescence maximum at 1540 nm does not depend on the content of Er or other components of the glass-forming matrix. The effective width $\Delta\lambda_{\text{eff}}$ of the spectra PL was calculated for these glasses according to the formula

$$\Delta\lambda_{\text{eff}} = \frac{\int I(\lambda)d\lambda}{I_{\text{max}}} \tag{1}$$

where $I(\lambda)$ is the emission intensity at wavelength λ and I_{max} is the maximum emission intensity.

The maximum $\Delta\lambda_{\text{eff}}$ value was found for the sample with 0.27 at.% Er (61 nm); this decreases the alloys with 0.16 at.% (52 nm) and 0.112 at.% Er (52 nm). The widening of the PL band in erbium-doped glasses was associated by the authors of [10] with the formation of clusters in the samples where $\text{Ga}/\text{Er} < 10$ is performed. Among the glassy alloys investigated here, the PL band widens in the sample with 0.27 at.% Er, and the above inequality is fulfilled. The microstructure study of alloys [11] showed the existence of inhomogeneities of 6–7 μm size the concentration of which increases with the amount of erbium. The generated inhomogeneities are

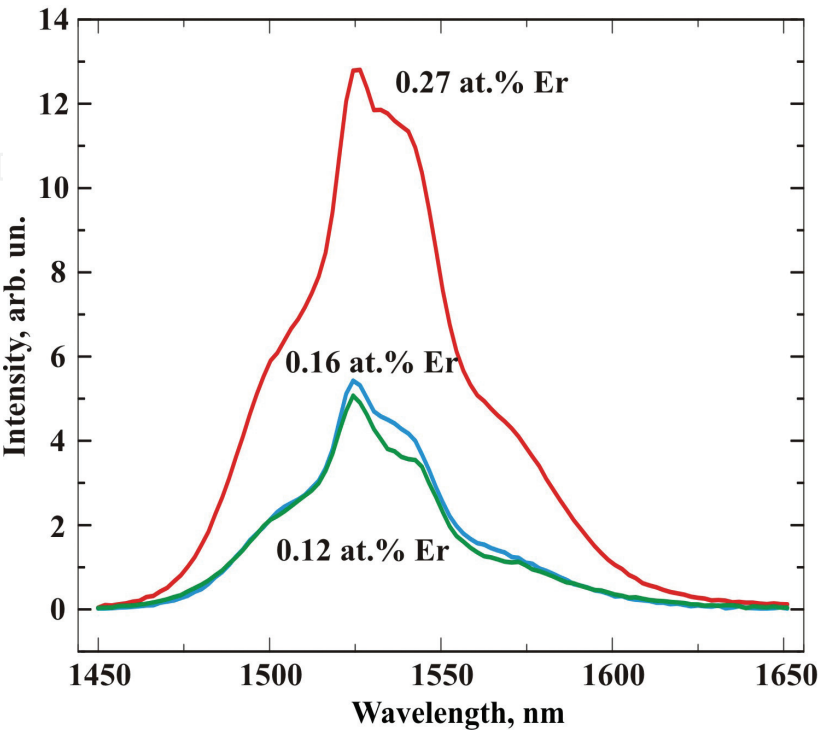


Figure 4.
Conversion FL spectra of the $\text{Ag}_{0.05}\text{Ga}_{0.05}\text{Ge}_{0.95}\text{S}_2 - \text{Er}_2\text{S}_3$ glasses.

good drains of defects which serve as the basis for cluster formation. Higher amounts of erbium favor the formation of clusters which include it. Thus, the PL intensity in the glasses is due to the emission of erbium ions which are uniformly distributed in the glass-forming matrix, as well as those which are located near the inhomogeneities and are involved in the formation of clusters. The study of static magnetization in the $\text{Ag}_{0.05}\text{Ga}_{0.05}\text{Ge}_{0.95}\text{S}_2\text{-Er}_2\text{S}_3$ glasses [12] confirmed the formation of clusters. The calculated number of erbium ions in the cluster was estimated there as $1\text{--}1.5 \times 10^3$.

The excitation at 980 nm yielded, in addition to the conversion PL (maximum at 1540 nm, **Figure 4**), the up-conversion PL bands in the visible and near-infrared spectral range at room temperature (**Figures 5 and 6**).

For all glasses, the luminescence is represented by three maxima at 520, 657, and 855 nm, which correspond to the radiative transitions $^2\text{H}_{11/2} \rightarrow ^4\text{I}_{15/2}$, $^4\text{F}_{9/2} \rightarrow ^4\text{I}_{15/2}$, and $^4\text{S}_{3/2} \rightarrow ^4\text{I}_{13/2}$ in Er^{3+} ions, respectively. In addition, a wide PL band in the range of 695–810 nm with an emission maximum at 765 nm was detected for the sample containing 0.27 at.% Er that cannot be interpreted by any radiative transition in erbium ion.

The intensity of the up-conversion PL bands depends on the laser excitation power (I_{IR}) which is expressed by the formula $I_{\text{PL}} \propto I_{\text{IR}}^n$, where n is the number of infrared photons per one PL photon. The number (n) can be found by the slope of the dependence of $\log(I_{\text{PL}})$ on $\log(I_{\text{IR}})$. PL spectral dependences for the sample with 0.27 at.% Er at different laser excitation powers are shown in **Figure 6**; these are also typical of the main maxima (520, 657, and 855 nm) in samples with less erbium content. The logarithmic dependence of the PL intensity on the excitation power [13], $\log(I_{\text{PL}})$ from $\log(P_{\text{IR}})$, is plotted in **Figure 7**.

Studies show that two photons with a wavelength of 980 nm are needed for the emission of one I_{PL} photon. An energy level diagram in erbium ions when excited by $h\nu_{980}$ quanta is shown in **Figure 8**. The absorption by the ground-state erbium ion of one $h\nu_{980}$ photon excites it to $^4\text{I}_{11/2}$ state. Such a transition can also take place via energy transfer (ET) from the neighboring excited erbium ion.

The excited state $^4\text{F}_{7/2}$ may be attained by the successive absorption of two $h\nu_{980}$ photons as well as by energy transfer to Er^{3+} ion in the $^4\text{I}_{11/2}$ state from another neighboring excited Er^{3+} ion [14]:

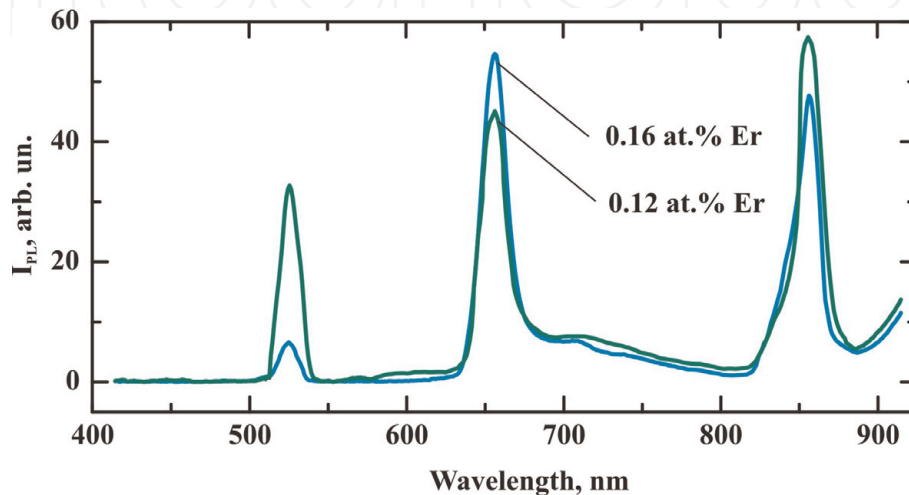
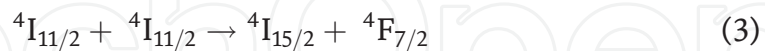


Figure 5.
Up-conversion PL spectra of the $\text{Ag}_{0.05}\text{Ga}_{0.05}\text{Ge}_{0.95}\text{S}_2\text{-Er}_2\text{S}_3$ glasses.

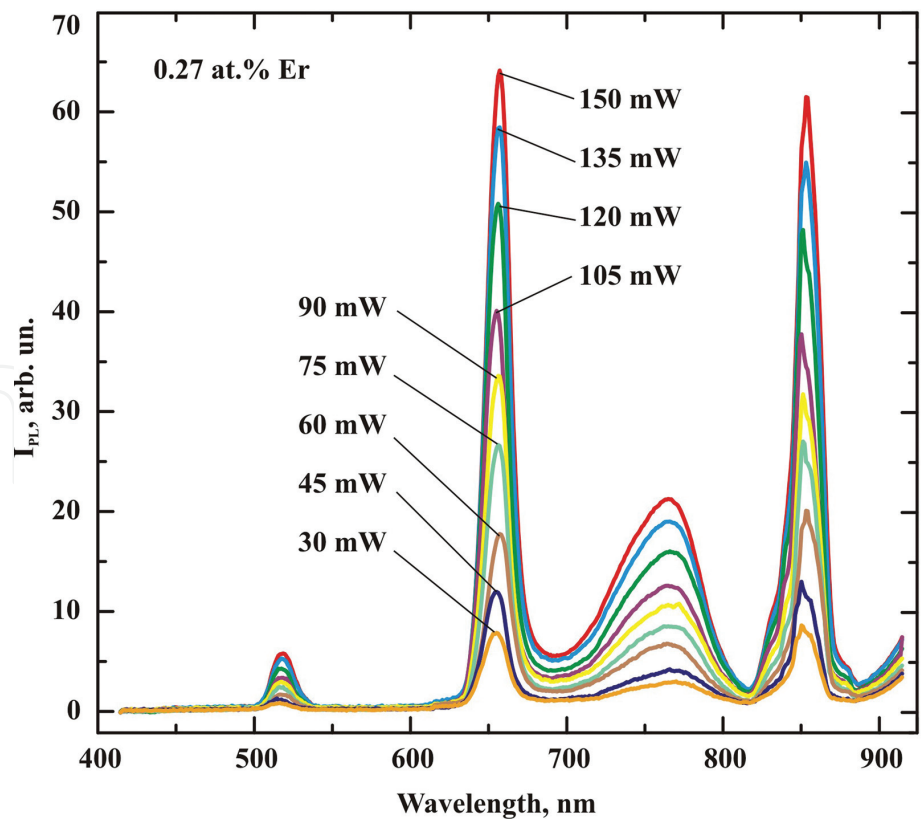


Figure 6.
Up-conversion FL spectra of the $\text{Ag}_{0.05}\text{Ga}_{0.05}\text{Ge}_{0.95}\text{S}_2\text{-Er}_2\text{S}_3$ glasses for various excitation power.

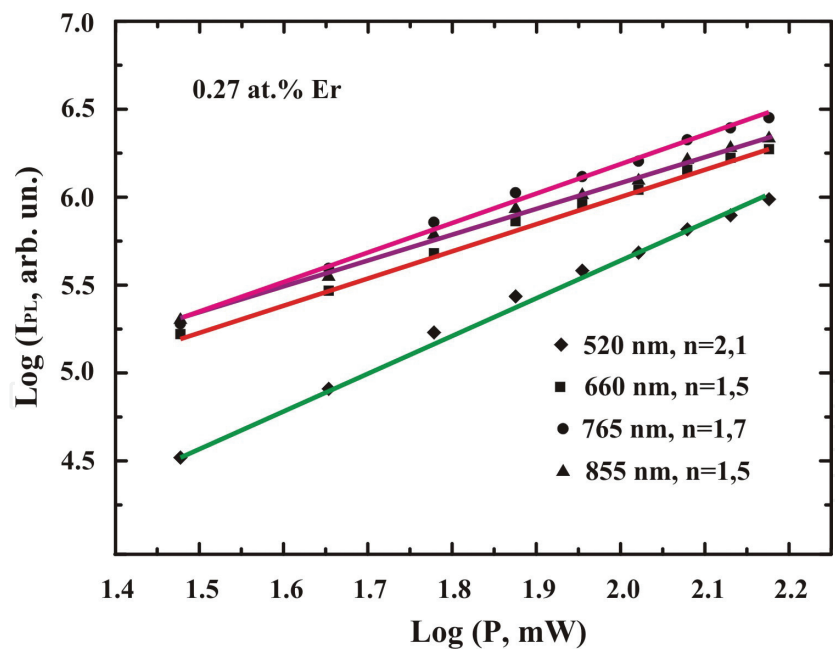


Figure 7.
Dependence of the luminescence intensity on the laser excitation power for the glass with 0.27 at.% Er.

The states $^2\text{H}_{11/2}$ and $^4\text{S}_{3/2}$ arise from non-radiative relaxation of the state $^4\text{F}_{7/2}$ due to the small energy distance between them. The non-radiative relaxation of Er^{3+} from the state $^4\text{S}_{3/2}$ to $^4\text{F}_{9/2}$ is unlikely due to large energy gap between them (about 3000 cm^{-1}) and low energy of phonons. According to Raman spectroscopy study, the energy of phonons for these glasses is close to $300\text{--}400\text{ cm}^{-1}$ [13]. Consequently, the state $^4\text{F}_{9/2}$ may arise by the absorption of the $h\nu_{980}$ photon

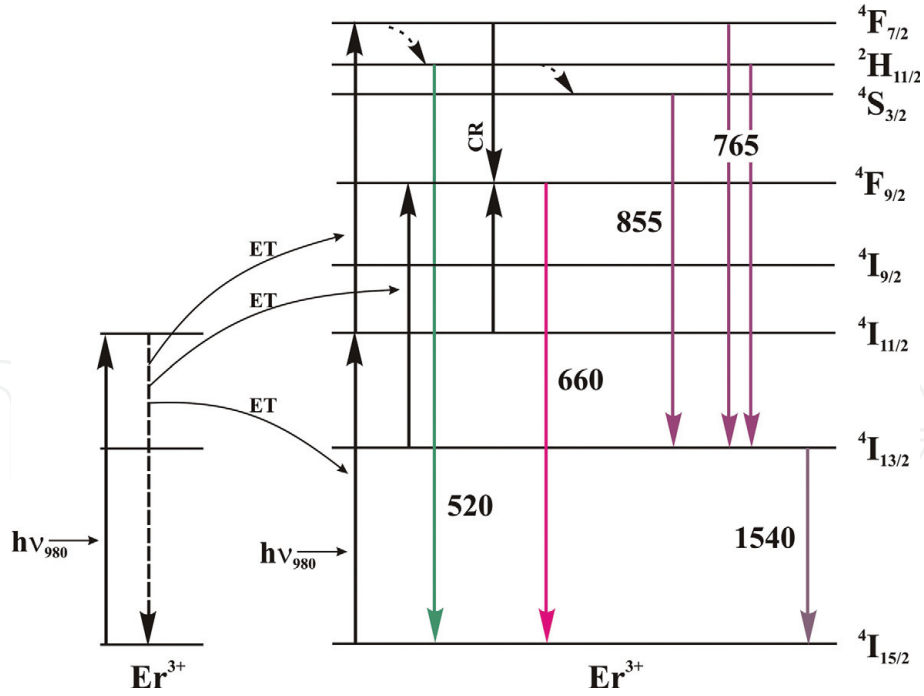


Figure 8.
Energy level diagram of erbium ions (for the $\text{Ag}_{0.05}\text{Ga}_{0.05}\text{Ge}_{0.95}\text{S}_2\text{-Er}_2\text{S}_3$ glasses, excitation by 980 nm).

(transition ${}^4\text{I}_{13/2} \rightarrow {}^4\text{F}_{9/2}$) or through the ET from the neighboring excited erbium ion. Additionally, the state ${}^4\text{F}_{9/2}$ state may appear due to cross-relaxation (CR):



Such a mechanism of occurrence of the excited state ${}^4\text{F}_{9/2}$ would explain the decrease in the intensity of the green (520 nm) and the amplification of the red PL band with an increase in the content of Er^{3+} ions when the distance between them decreases and the conditions favor ET.

The increase of PL intensity in the chalcogenide glasses may be due to the increase in erbium content and the change in the composition of the glass-forming matrix. It should be noted that an increase in erbium content in glasses can lead to the concentration quenching of PL [15] as well as to the crystallization of the host. Therefore, increasing the PL efficiency requires the selection of optimal composition of the glass-forming matrix and adding into its composition the maximum concentration of erbium that will not cause PL quenching and the crystallization of glass. The choice of the components of the glass-forming matrix should take into account their glass-forming ability and the ability of sustaining large amount of REs and also maintaining a wide transparency window in the visible and infrared range when adding admixtures. With the above considerations, the $\text{Ga}_2\text{S}_3\text{-La}_2\text{S}_3\text{-Er}_2\text{S}_3$ system is of interest, in our opinion. Using the technique in paragraph. 2, we successfully introduced up to 40 mol.% La_2S_3 and 3 mol.% Er_2S_3 into the glass. The shift of the optical absorption edge does not exceed 0.13 eV with Er_2S_3 doping and 0.10 eV with the addition of 30–40 mol.% La_2S_3 [16]. Thus, the luminescence properties of the $\text{Ga}_2\text{S}_3\text{-La}_2\text{S}_3\text{-Er}_2\text{S}_3$ system glasses at room temperature and 80 K were investigated with a considerable variation in the host composition. The component composition of the glasses is listed in **Table 1**.

Photoluminescence spectra in the 480–1700 nm range upon laser excitation at 488 nm wavelength at 80 K are shown in **Figures 9 and 10**. The intense maxima at 550, 855, 985, 1100, and 1540 nm correspond to 4f intra-shell transitions ${}^4\text{S}_{3/2} \rightarrow {}^4\text{I}_{15/2}$, ${}^4\text{S}_{3/2} \rightarrow {}^4\text{I}_{13/2}$, ${}^4\text{I}_{11/2} \rightarrow {}^4\text{I}_{15/2}$, ${}^2\text{H}_{11/2} \rightarrow {}^4\text{I}_{11/2}$, ${}^4\text{I}_{13/2} \rightarrow {}^4\text{I}_{15/2}$ in Er^{3+} ions.

| Sample no. | Ga ₂ S ₃ | La ₂ S ₃ | Er ₂ S ₃ |
|------------|--------------------------------|--------------------------------|--------------------------------|
| | (mol. %) | | |
| 1 | 64 | 35 | 1 |
| 2 | 62 | 35 | 3 |
| 3 | 59 | 40 | 1 |
| 4 | 57 | 40 | 3 |

Table 1.
Component composition of the Ga₂S₃-La₂S₃-Er₂S₃ glasses.

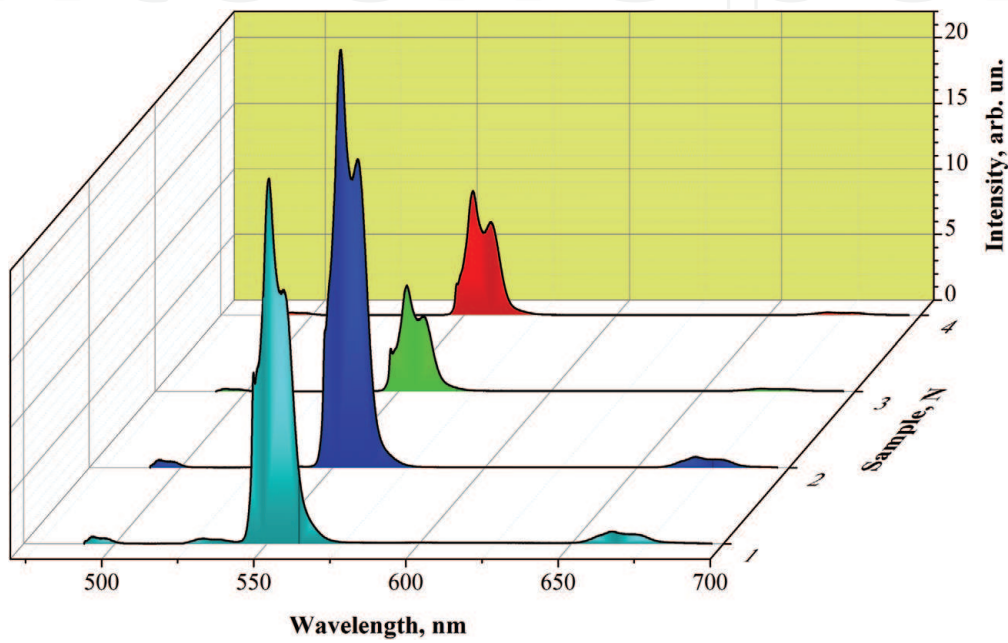


Figure 9.
PL spectra of the Ga₂S₃-La₂S₃-Er₂S₃ glasses at 80 K (visible range).

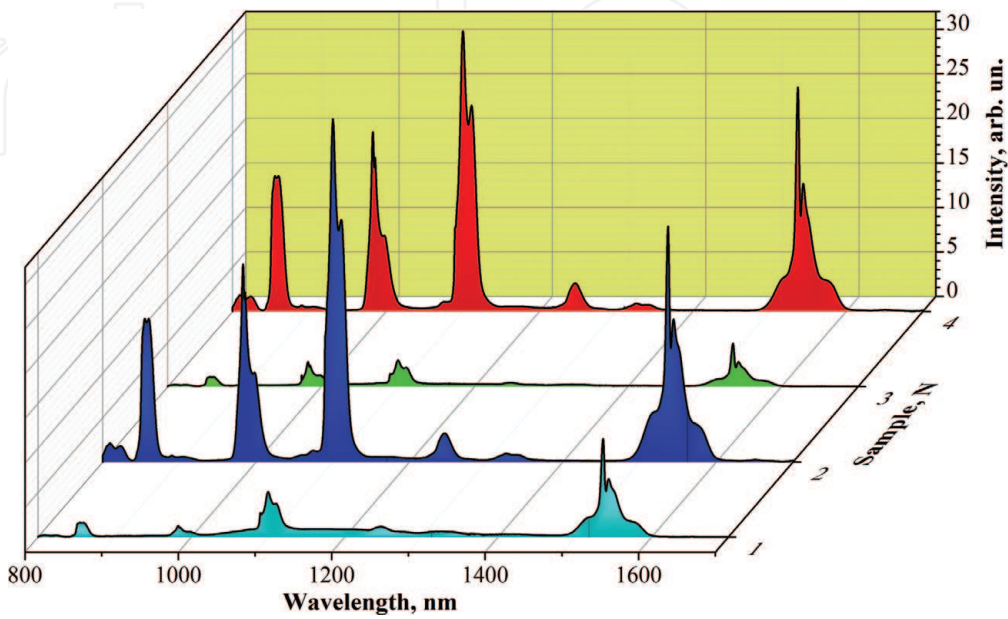


Figure 10.
PL spectra of the Ga₂S₃-La₂S₃-Er₂S₃ glasses at 80 K (infrared range).

The lower-intensity maxima at 492, 660, 810, and 1245 nm correspond to the transitions $^4F_{7/2} \rightarrow ^4I_{15/2}$, $^4F_{9/2} \rightarrow ^4I_{15/2}$, $^4I_{9/2} \rightarrow ^4I_{15/2}$, $^4F_{7/2} \rightarrow ^4I_{9/2}$ in erbium ions, respectively.

PL intensity increases in the visible and infrared ranges with Er_2S_3 concentration at constant content of La_2S_3 . The best medium for PL (the most intense PL) is the glass-forming matrix with 35 mol.% La_2S_3 and 3 mol.% Er_2S_3 . PL intensity decreases when La_2S_3 content increased to 40 mol.%. A similar effect was observed by Ivanova in [17] in the glasses of the GeS_2 - Ga_2S_3 system, explaining this by an increase in the number of homopolar metallic bonds. It is likely that the number of La-La-type bonds increases in the Ga_2S_3 - La_2S_3 - Er_2S_3 glasses with increasing La_2S_3 content.

Changing the component composition of glass leads to redistribution of the intensity of PL bands. The maximum at 550 nm is dominating in the visible range, and its intensity decreases with increasing La_2S_3 content. The greatest increase in the intensity of PL bands occurs for the infrared spectral range with an increase in erbium concentration. The changes in the PL spectra are clearly related to the mechanism of the realization of excited states in Er^{3+} ions.

The redistribution of the PL intensity is due to the competing ways of achieving excited states in erbium ions. **Figure 11** shows an energy level diagram of erbium ions [18] which reveals the mechanism of PL emission in the glasses of the Ga_2S_3 - La_2S_3 - Er_2S_3 system. Accordingly, erbium ions jump from the ground to the excited state of $^4F_{7/2}$ upon excitation by 488 nm wavelength. Intense emission of green and infrared light (550, 1100, and 855 nm) results when the majority of erbium ions non-radiatively relax to the states $^2H_{11/2}$ and $^4S_{3/2}$. Only a small fraction of erbium undergoes transitions $^4F_{7/2} \rightarrow ^4I_{15/2}$ and $^4F_{7/2} \rightarrow ^4I_{9/2}$ as PL bands at 492 and 1245 nm are characterized by low intensity. Additionally, PL with a maximum at 660 nm occurs due to the cross-relaxation process CR resulting in the excited state $^4F_{9/2}$.

PL spectra of the Ga_2S_3 - La_2S_3 - Er_2S_3 glasses at room temperature are shown in **Figures 12** and **13**. Compared to the spectra at 80 K, the PL intensity at 530 nm increased slightly (transition $^2H_{11/2} \rightarrow ^4I_{15/2}$), and the band intensity at 660 nm increased (transition $^4F_{9/2} \rightarrow ^4I_{15/2}$). Additionally, the intensity of the maxima of

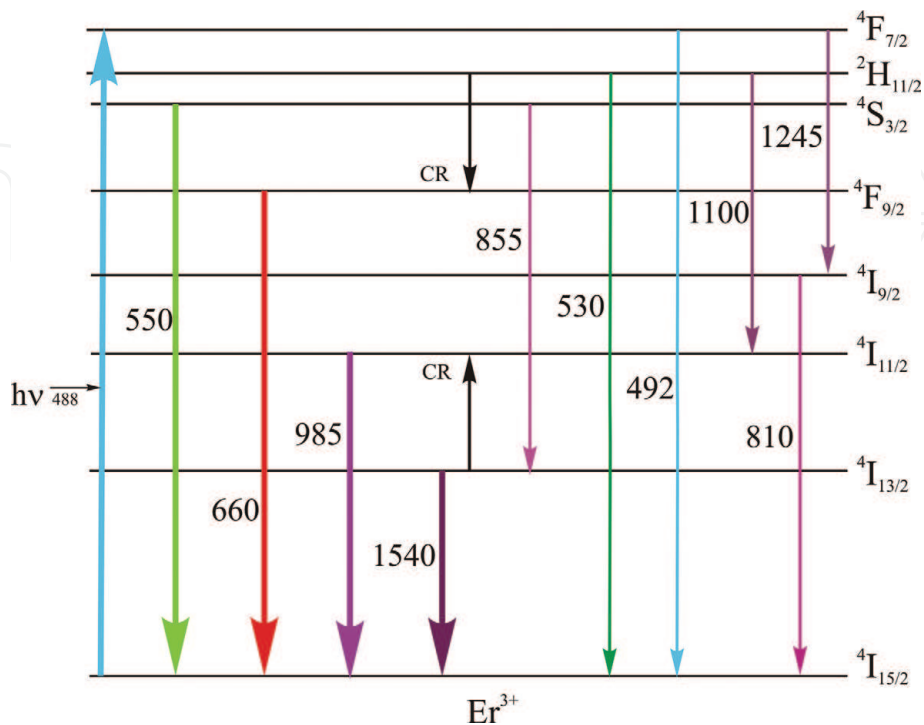


Figure 11.
Energy level diagram of erbium ions (for the Ga_2S_3 - La_2S_3 - Er_2S_3 glasses).

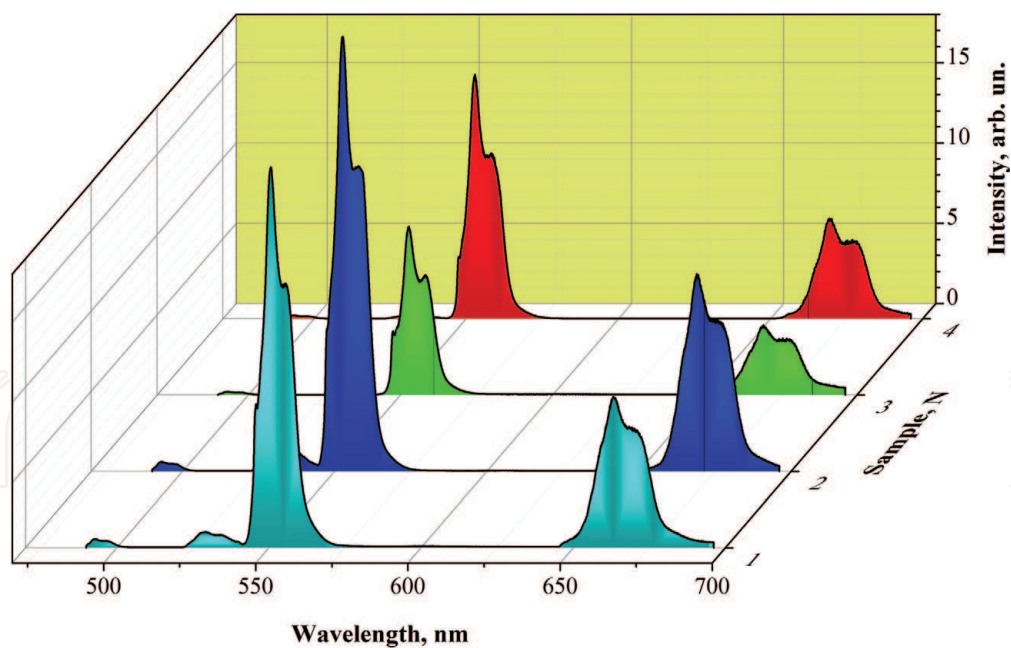


Figure 12.
 PL spectra of the $\text{Ga}_2\text{S}_3\text{-La}_2\text{S}_3\text{-Er}_2\text{S}_3$ glasses at room temperature (visible range).

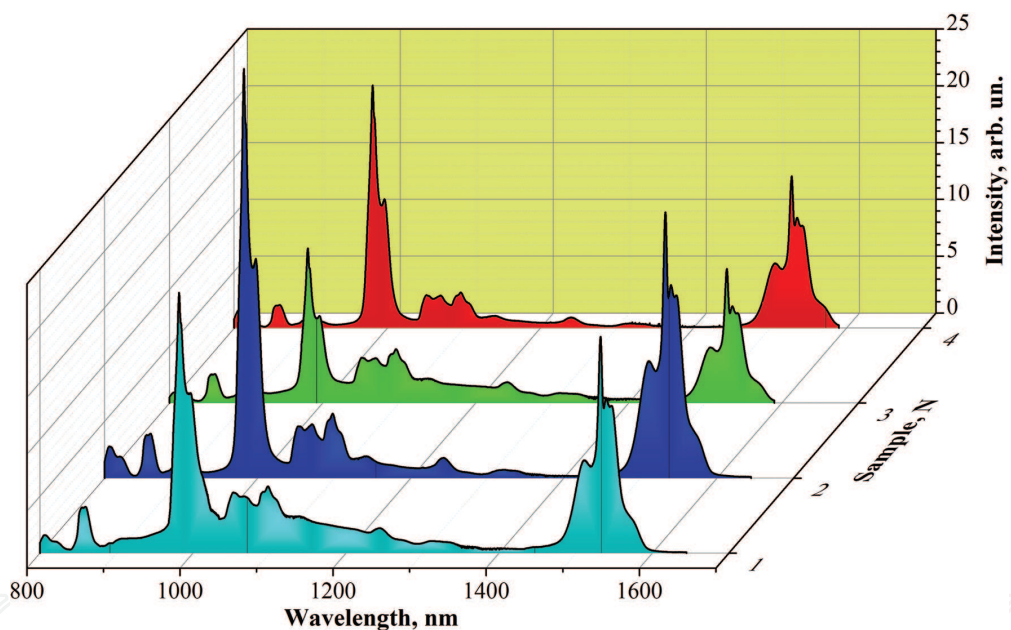


Figure 13.
 PL spectra of the $\text{Ga}_2\text{S}_3\text{-La}_2\text{S}_3\text{-Er}_2\text{S}_3$ glasses at room temperature (infrared range).

1100 and 855 nm significantly decreased, and a weak PL band at 1050 nm was observed in the infrared spectral range. Such intensity redistribution of the PL maxima is associated with a change in the concentration of erbium ions in different excited states. This is related to the fact that when the temperature rises, the phonon subsystem of the glass-forming matrix is transformed, so the probability of the energy exchange of the neighboring erbium ions increases. As a result, the role of cross-relaxation processes increases and the number of erbium ions in the state $^4\text{F}_{9/2}$ increases. Thus the intensity of the PL band with a maximum at 660 nm increases. Additionally, CR affects the decrease of the number of erbium ions in the states $^2\text{H}_{11/2}$ and $^4\text{S}_{3/2}$ leading to the decrease of the intensity of the maxima at 1100 and 855 nm at room temperature. The band with a maximum at 1050 nm (transition $^4\text{F}_{3/2} \rightarrow ^4\text{I}_{9/2}$) is completely overlapped by the intense PL maximum at 1100 nm at 80 K.

4. Photoluminescence in erbium-doped single crystals

The occurrence of recombination PL that is characterized by wide emission bands in the visible, rarely in the infrared range, is quite often found in single-crystalline chalcogenide semiconductors at room temperature or low temperatures [19, 20]. From the application viewpoint of laser technology and telecommunications, the introduction of erbium to such materials has significant advantages since the emission bands of erbium-doped glasses and single crystals are usually intense and narrow. The addition of erbium is also accompanied by the extinction of PL radiation [21] which is due to the crystalline or amorphous chalcogenide host. The influence of external factors on the PL efficiency in erbium-doped chalcogenides is limited due to the shielding of radiative transitions in the 4f-shell of Er by outer shells. At the same time, the local environment of erbium ion, both in glasses and single crystals, affects the efficiency of PL emission which is why it is extremely important for the design of fluorescent materials. It should be noted that the single crystals, unlike glasses, do not permit a wide variation of the component composition since it is limited by the solid solubility of impurities and the homogeneity of the crystalline compound. It is more difficult to select the composition of the host to obtain effective emission in erbium-doped single crystals; therefore, PL is less common in these than in the corresponding amorphous media.

The investigation of the optical properties of the single crystals $(\text{Ga}_{55}\text{In}_{45})_2\text{S}_{300}$ and $(\text{Ga}_{54.59}\text{In}_{44.66}\text{Er}_{0.75})_2\text{S}_{300}$ [7] determined that the introduction of erbium does not result in a change in the bandgap energy or significant changes in the electronic structure [22]. The absorption maxima at 530, 660, 810, 980, and 1530 nm [7] recorded for $(\text{Ga}_{54.59}\text{In}_{44.66}\text{Er}_{0.75})_2\text{S}_{300}$ single crystal correspond to 4f intra-shell transitions from the ground state to the excited states $^2\text{H}_{11/2}$, $^4\text{F}_{9/2}$, $^4\text{I}_{9/2}$, $^4\text{I}_{11/2}$, and $^4\text{I}_{13/2}$ in Er^{3+} ions, respectively. PL spectra at room temperature in the visible and close infrared range (600–1650 nm) were studied when excited by a laser with 532 nm wavelength (**Figure 14**). Two intense PL bands with maxima at 810 and 1540 nm were recorded, which correspond to the transitions of $^4\text{I}_{9/2} \rightarrow ^4\text{I}_{15/2}$ and $^4\text{I}_{13/2} \rightarrow ^4\text{I}_{15/2}$ in Er^{3+} ions, respectively.

Er^{3+} ions excited by a 532 nm laser are promoted from the ground $^4\text{I}_{15/2}$ to the excited state $^2\text{H}_{11/2}$. The emission mechanism in this case is quite simple as demonstrated at an energy transition diagram in erbium ions (**Figure 15**). Erbium ions cannot relax non-radiatively from the state $^4\text{S}_{3/2}$ to $^4\text{F}_{9/2}$ or $^4\text{I}_{9/2}$ due to the large energy distance and the low phonons energy ($200\text{--}300\text{ cm}^{-1}$ for the single crystals $(\text{Ga}_{55}\text{In}_{45})_2\text{S}_{300}$ and $(\text{Ga}_{54.59}\text{In}_{44.66}\text{Er}_{0.75})_2\text{S}_{300}$ [23]). Therefore, the appearance of

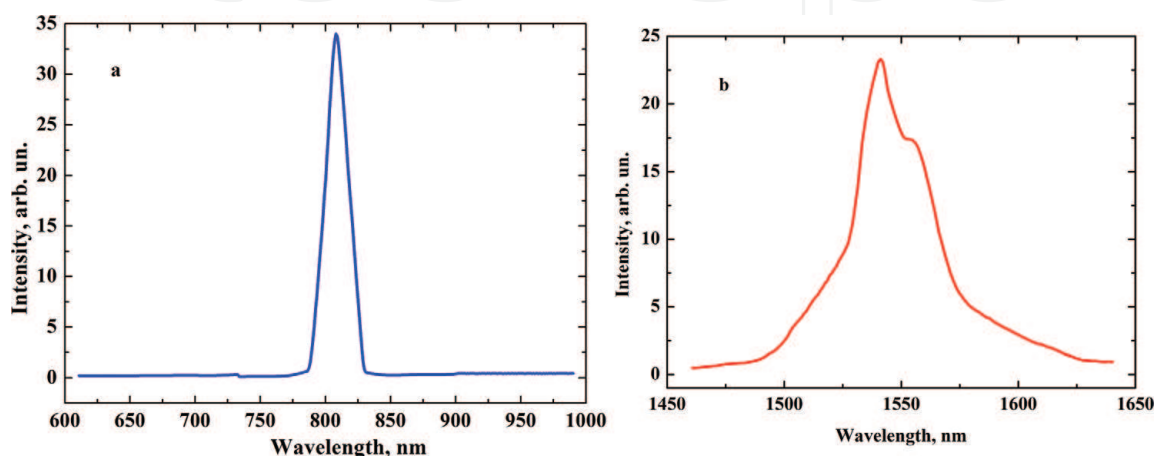


Figure 14. Visible (a) and NIR (b) PL spectra of the $(\text{Ga}_{54.59}\text{In}_{44.66}\text{Er}_{0.75})_2\text{S}_{300}$ single crystal (excitation by 532 nm).

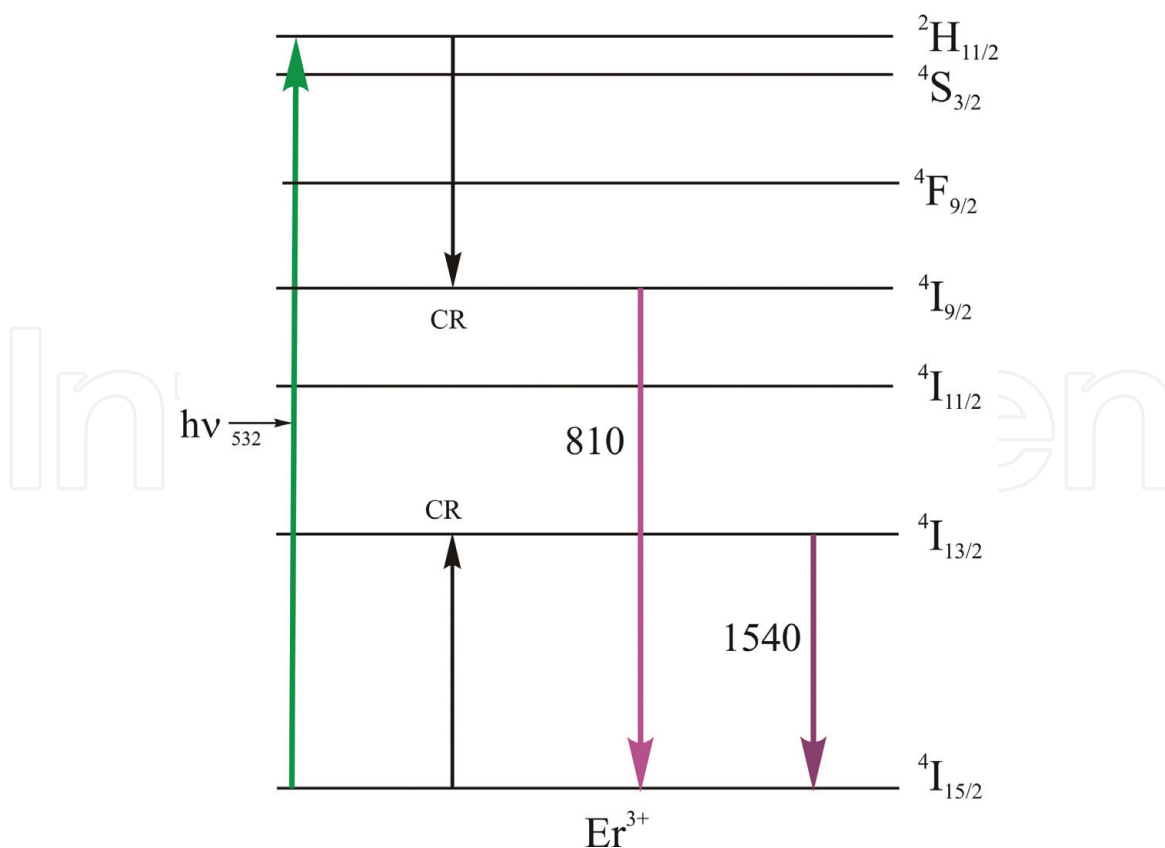
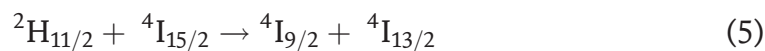


Figure 15.
Energy level diagram in erbium ions (for a $(\text{Ga}_{54.59}\text{In}_{44.66}\text{Er}_{0.75})_2\text{S}_{300}$ single crystal, excitation by 532 nm).

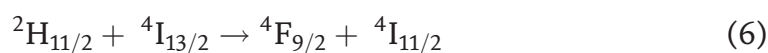
excited states $^4\text{I}_{9/2}$ involves the cross-relaxation process CR. Energy transfer between adjacent erbium ions in the states $^2\text{H}_{11/2}$ and $^4\text{I}_{15/2}$ promotes one ion into the excited state $^4\text{I}_{9/2}$ and the other into $^4\text{I}_{13/2}$:



Such a mechanism yields substantial numbers of erbium ions in excited states $^4\text{I}_{9/2}$ and $^4\text{I}_{13/2}$, which results in PL with maxima at 810 and 1540 nm.

Similar to glasses, we also investigated single crystals in which two rare earth metals were introduced. $(\text{Ga}_{55}\text{In}_{45})_2\text{S}_{300}$ and $(\text{Ga}_{54.59}\text{In}_{44.66}\text{Er}_{0.75})_2\text{S}_{300}$ single crystals were obtained by a solution-melt method [24] selected in accordance with the phase diagram of the $\text{Ga}_2\text{S}_3\text{-La}_2\text{S}_3$ system. The bandgap energy of the single crystals little changes upon erbium doping at 2.01 and 1.99 eV for $(\text{Ga}_{55}\text{In}_{45})_2\text{S}_{300}$ and $(\text{Ga}_{54.59}\text{In}_{44.66}\text{Er}_{0.75})_2\text{S}_{300}$, respectively [24]. PL of $(\text{Ga}_{54.59}\text{In}_{44.66}\text{Er}_{0.75})_2\text{S}_{300}$ single crystal in the 500–1700 nm range was investigated at room temperature (**Figure 16**). Four intense PL bands with maxima at 525, 545, 980, and 1540 nm and one low-intensity band at 660 nm were recorded. They correspond to the transitions in Er^{3+} ions from excited states $^2\text{H}_{11/2}$, $^4\text{S}_{3/2}$, $^4\text{I}_{11/2}$, $^4\text{I}_{13/2}$, and $^4\text{F}_{9/2}$ to the ground state.

Energy transition diagram (**Figure 17**) shows that the wavelength of 810 nm can excite erbium ions from the ground state $^4\text{I}_{15/2}$ to the state $^4\text{I}_{9/2}$. Er^{3+} ions, either by directly absorbing light quanta or through ET, can be promoted from the state $^4\text{I}_{13/2}$ to $^2\text{H}_{11/2}$ resulting in PL at 525 nm. Additionally, after non-radiative relaxation of erbium ions to the state $^4\text{S}_{3/2}$, there is a PL band with a maximum at 545 nm [25]. The appearance of excited states $^4\text{F}_{9/2}$ and $^4\text{I}_{11/2}$ occurs by cross-relaxation CR 2:



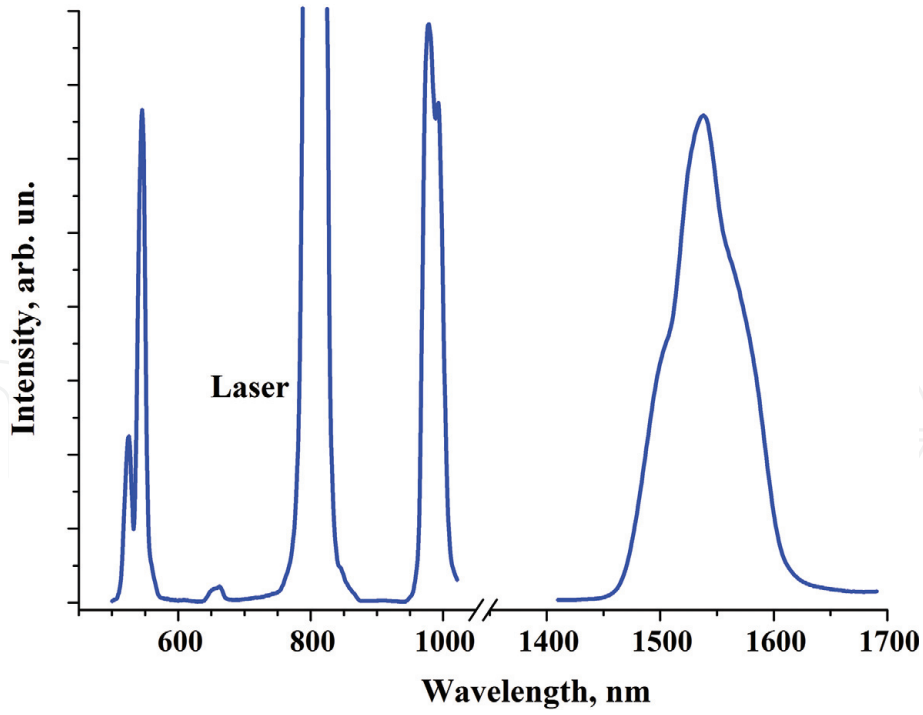


Figure 16.
PL of the $(\text{Ga}_{69.75}\text{La}_{29.75}\text{Er}_{0.5})_2\text{S}_{300}$ single crystal (excitation by 810 nm).

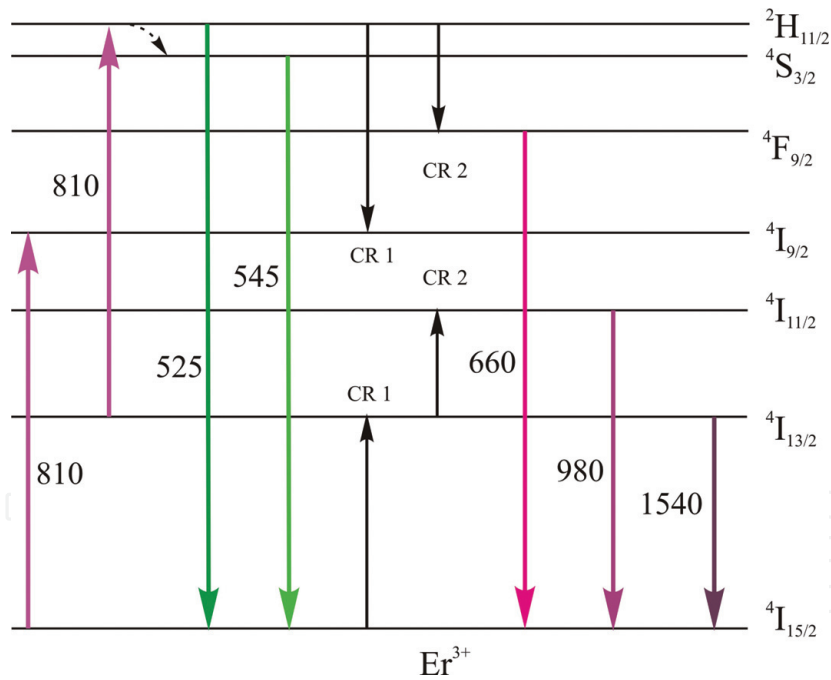
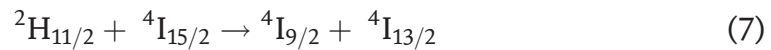


Figure 17.
Energy level diagram in erbium ions (for a $(\text{Ga}_{69.75}\text{La}_{29.75}\text{Er}_{0.5})_2\text{S}_{300}$ single crystal, excitation by 810 nm).

The transition from these states to the ground state produces PL at 660 and 980 nm. An intense PL band at 1540 nm wavelength occurs due to the formation of a significant number of Er^{3+} ions in the state $^4\text{I}_{13/2}$ by cross-relaxation CR 1:



The excitation of the single crystal yields also an intense up-converted green PL (**Figure 16**). Therefore, $(\text{Ga}_{54.59}\text{In}_{44.66}\text{Er}_{0.75})_2\text{S}_{300}$ single crystal can be recommended as a material for the manufacture of light converters.

5. The influence of temperature on the photoluminescent properties of glasses and crystals

Doping the binary and ternary chalcogenides, particularly by rare earth metals, creates materials for the design of active and passive media for laser technology, photonic devices, light converters, and telecommunications. Special attention is given to the crystalline and amorphous environments that can exhibit high-intensity PL under the influence of external factors.

Additionally, modern optoelectronic industry actively researches and implements high-precision temperature sensors based on the sensitivity of PL emission to temperature changes. The design of such devices requires the investigation of the effect of temperature on the mechanism of the achievement of excited states and the processes of the relaxation of erbium ions when the PL intensity changes in various temperature ranges. This will allow optimizing the component composition of crystals and glasses to produce effective luminescent materials for the development of non-contact optical sensors.

PL of the $\text{Ag}_{0.05}\text{Ga}_{0.05}\text{Ge}_{0.95}\text{S}_2\text{-Er}_2\text{S}_3$ glasses in 600–1050 nm range was investigated in a temperature range of 80–300 K upon laser excitation at 532 nm [26]. Recorded PL bands with maxima at 660, 860, and 980 nm correspond to the radiative transitions $^4\text{F}_{9/2} \rightarrow ^4\text{I}_{15/2}$, $^4\text{S}_{3/2} \rightarrow ^4\text{I}_{13/2}$, $^4\text{I}_{11/2} \rightarrow ^4\text{I}_{15/2}$ in erbium ions, respectively. The dependences of PL intensity on wavelength at different temperatures for the sample with 0.27 at.% Er are plotted in **Figure 18** (also typical of the glasses with 0.12, 0.16 at.% Er). The temperature increase leads to changes in the ratio of PL intensities, with the intensity of all bands decreasing at temperatures above 180 K. The PL band with a maximum at 860 nm is the most sensitive to temperature changes. The PL emission mechanism is well explained by the energy level diagram of Er^{3+} ions (**Figure 19**).

Illumination by 532 nm wavelength promotes erbium ions to the excited state $^2\text{H}_{11/2}$. The states $^4\text{F}_{9/2}$, $^4\text{I}_{9/2}$, and $^4\text{I}_{11/2}$ result in the cross-relaxation processes CR1, CR2, and CR3. Er^{3+} ions in the $^2\text{H}_{11/2}$ state can also nonradiatively relax to the $^4\text{S}_{3/2}$ state due to small energy gap between them. The integral intensity of the emission bands was calculated from the results of the investigation of PL spectra.

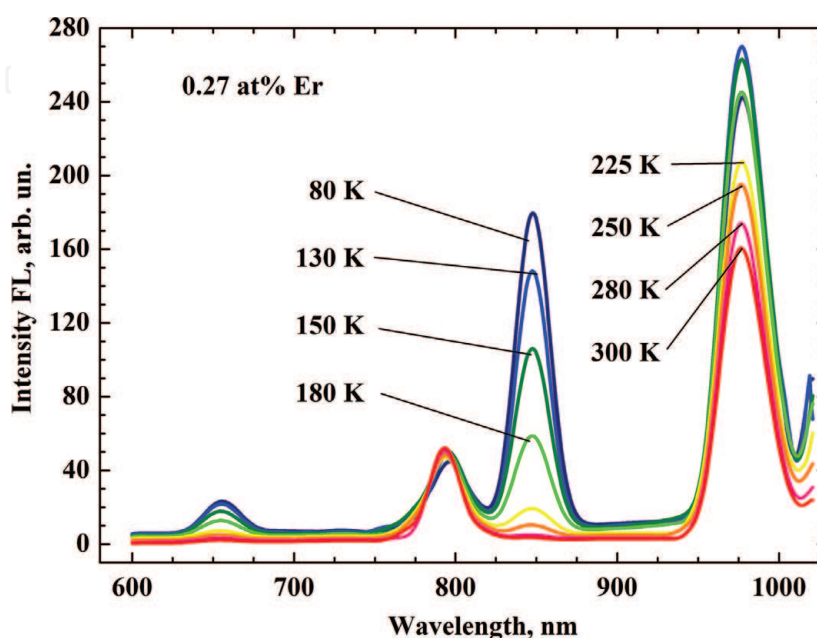


Figure 18.
 PL spectra of the $\text{Ag}_{0.05}\text{Ga}_{0.05}\text{Ge}_{0.95}\text{S}_2\text{-Er}_2\text{S}_3$ glass (0.27 at.% Er) at various temperatures.

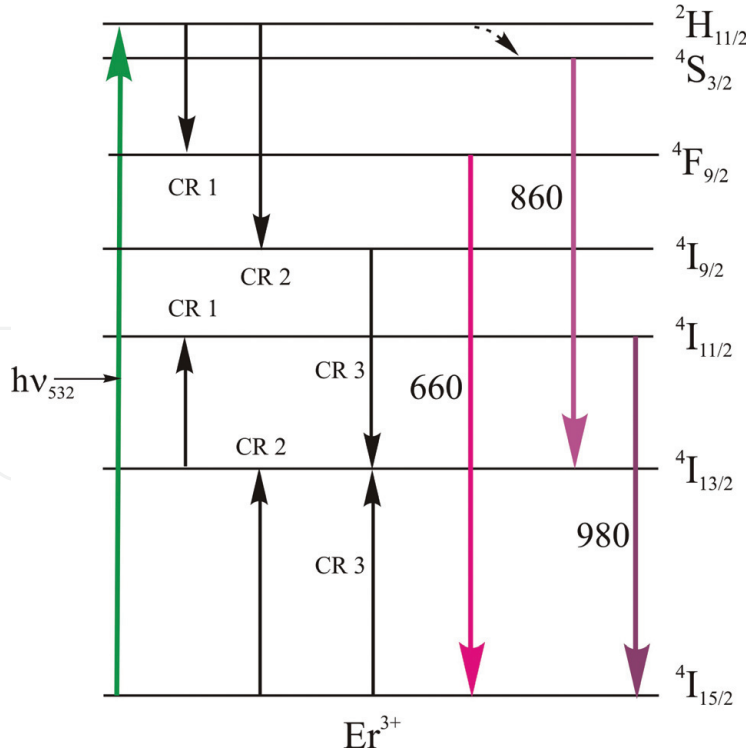


Figure 19.

Energy level diagram in erbium ions (for the $\text{Ag}_{0.05}\text{Ga}_{0.05}\text{Ge}_{0.95}\text{S}_2\text{-Er}_2\text{S}_3$ glasses, excitation by 532 nm).

The dependence of integral PL intensity on temperature is shown in **Figure 20** for the glass with 0.27 at.% Er.

The dependence of PL intensity on temperature can be described using the probability of radiative and non-radiative processes by the formula [27]:

$$I(T) = \frac{I_0}{1 + \frac{\omega_{nr}}{\omega_r} \exp\left(-\frac{E_t}{kT}\right)} \quad (8)$$

where I_0 is a constant, k is Boltzmann's constant, ω_{nr} , ω_r is the probability of non-radiative and radiative processes, respectively, and E_t is the thermal activation energy of luminescence.

The $I(T)$ dependence (**Figure 20**, solid line) was calculated from Eq. (8) for the band with the 860 nm maximum, and the corresponding activation energy E_t was calculated as 90 ± 6 meV [26]. According to the diagram in **Figure 19**, this energy determines the activation of erbium ions from the state $^4\text{S}_{3/2}$ or $^2\text{H}_{11/2}$ (i.e., the energy gap between these states). It should be noted that changes in PL intensity is complex. Therefore we calculated the logarithm of the ratio of integral PL intensities $\ln(I_{980}/I_{660})$ and plotted its dependence on temperature (**Figure 21**). This dependence is linear in the range of 125–300 K. The sensitivity of the sample as the temperature sensor was calculated according to the results of these studies as 0.43 K^{-1} .

Erbium-doped single crystals may also exhibit changes of PL intensity with temperature. PL spectra of the single crystal $(\text{Ga}_{54.59}\text{In}_{44.66}\text{Er}_{0.75})_2\text{S}_{300}$ were investigated at 150, 200, 250, and 300 K upon laser excitation at 980 nm wavelength (**Figures 22 and 23**). The position and shape of the maxima do not change but the intensity of PL increases with temperature. For the majority of semiconductor

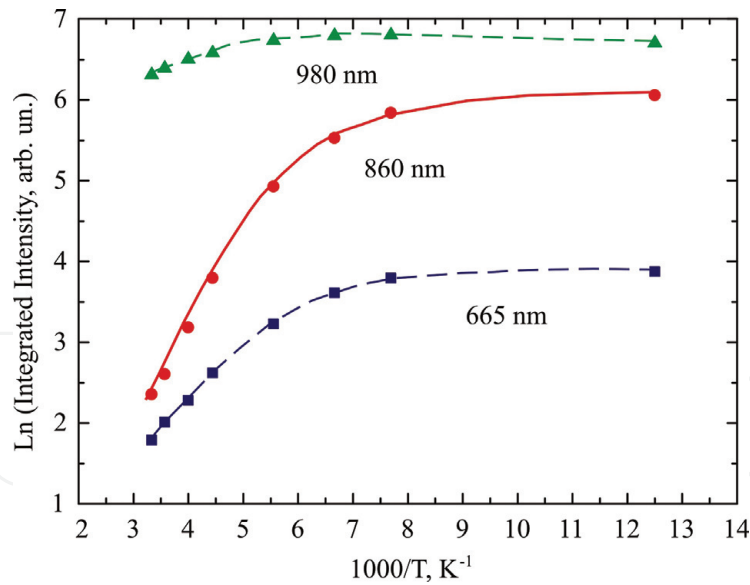


Figure 20.
Temperature dependence of integral PL intensity of the $Ag_{0.05}Ga_{0.05}Ge_{0.95}S_2-Er_2S_3$ glass (0.27 at.% Er).

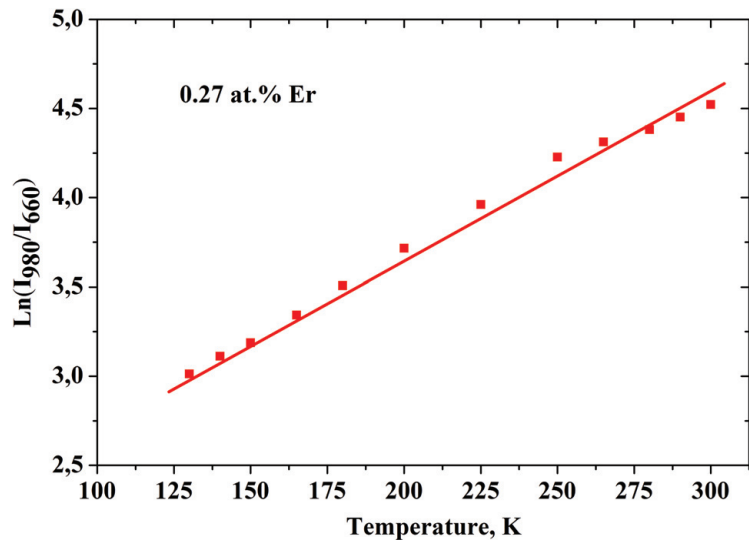
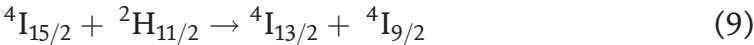


Figure 21.
Ratio of integral PL intensity of the glasses of the $Ag_{0.05}Ga_{0.05}Ge_{0.95}S_2-Er_2S_3$ system (0.27 at.% Er).

materials where the recombination luminescence was recorded [28], the PL intensity decreases with increasing temperature. At the same time, the emission intensity may increase with temperature in crystals and glasses where PL is associated with transitions in the 4f-shell of erbium ions. This is due to the fact that the neighboring erbium ions are in different excited states. As the temperature increases, the phonon subsystem of the crystal changes which contributes to the cross-relaxation processes of Er^{3+} ions. If a crystal is excited by 980 nm wavelength, the absorption of two photons promotes erbium ion into the state $^4F_{7/2}$ (Figure 22). Due to small energy gap, Er^{3+} ions can non-radiatively relax to the state $^2H_{11/2}$. Excited states $^4I_{13/2}$ and $^4I_{9/2}$ result from the CR process:



Therefore, CR processes play greater role with increasing temperature, which will contribute to a higher concentration of erbium ions in the $^4I_{9/2}$ and $^4I_{13/2}$ states and the increase in PL intensity.

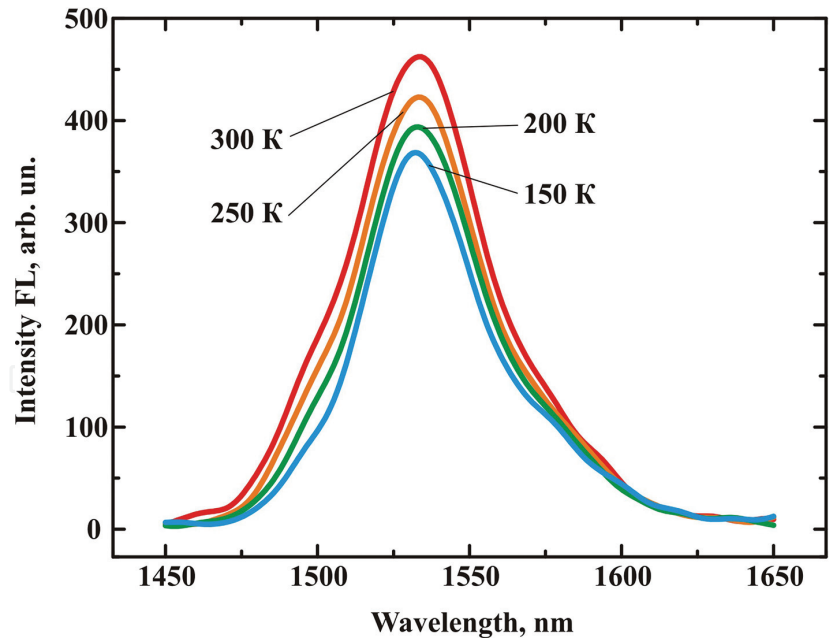


Figure 22.
Conversion PL spectra of the $(\text{Ga}_{54.59}\text{In}_{44.66}\text{Er}_{0.75})_2\text{S}_{300}$ single crystal at various temperatures.

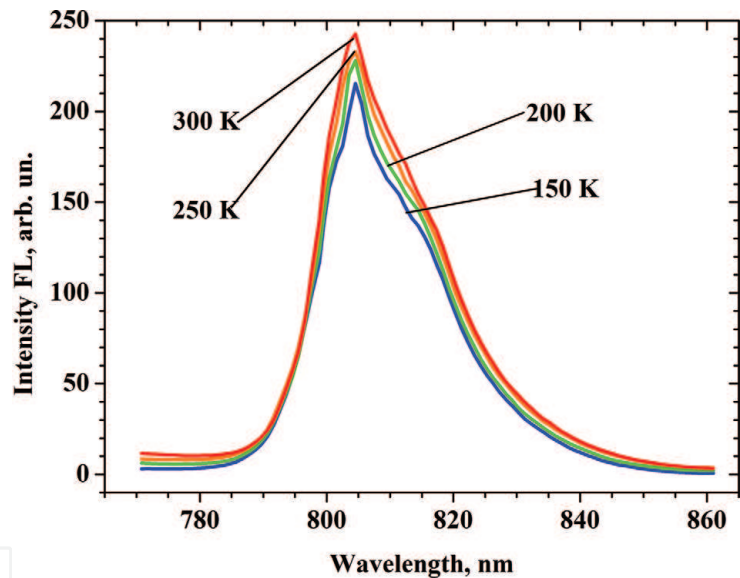


Figure 23.
Up-conversion PL spectra of the $(\text{Ga}_{54.59}\text{In}_{44.66}\text{Er}_{0.75})_2\text{S}_{300}$ single crystal at various temperatures.

The integral PL intensity for both maxima was calculated from the spectra of up-conversion and conversion PL of $(\text{Ga}_{54.59}\text{In}_{44.66}\text{Er}_{0.75})_2\text{S}_{300}$ single crystal (**Figure 24**). The plots of integral PL intensity linearly depend on temperature. From the results of the temperature dependence of the integral PL intensity, the sensitivity was calculated as $1.187 \times 10^{-3} \text{ K}^{-1}$ for PL at 805 nm and $1.818 \times 10^{-3} \text{ K}^{-1}$ for the maximum at 1540 nm. It should be noted that the sensitivity defined as the ratio of the integral intensities of the two PL bands is higher in the $\text{Ag}_{0.05}\text{Ga}_{0.05}\text{Ge}_{0.95}\text{S}_2\text{-Er}_2\text{S}_3$ glasses. The sensitivity in $(\text{Ga}_{54.59}\text{In}_{44.66}\text{Er}_{0.75})_2\text{S}_{300}$ single crystal was calculated separately for each PL band (maxima at 805 and 1540 nm), the latter being in the operating range of fiber-optical networks and telecommunication devices.

Therefore, in a limited temperature range, the $\text{Ag}_{0.05}\text{Ga}_{0.05}\text{Ge}_{0.95}\text{S}_2\text{-Er}_2\text{S}_3$ glasses (with 0.27 at.% Er) and the single crystals $(\text{Ga}_{54.59}\text{In}_{44.66}\text{Er}_{0.75})_2\text{S}_{300}$ can be used to design non-contact optical temperature sensors.

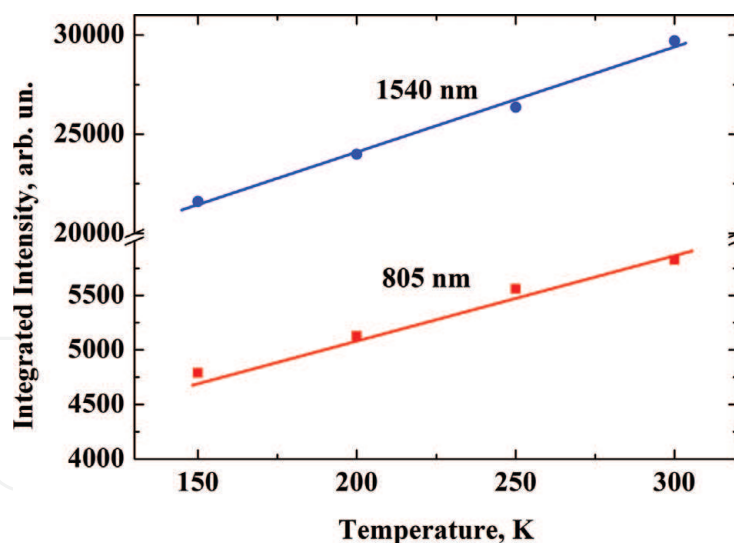


Figure 24.
Temperature dependence of integral PL intensity of the $(\text{Ga}_{54.59}\text{In}_{44.66}\text{Er}_{0.75})_2\text{S}_{300}$ single crystal.

6. Conclusions

The principal mechanisms of the occurrence of PL due to the transitions in the 4f-shell of erbium ions are presented on the basis of sulfide glasses and single crystals. The appearance of many emission bands in chalcogenide glasses (unlike single crystals) is due to the fact that in an amorphous medium, erbium ions may occupy several different positions in the glass-forming matrix. The change of the excitation wavelength leads to a change in the mechanism for the excited states in Er^{3+} ions and the emergence of some radiation bands and the extinction of others. Energy exchange processes (energy transfer, cross-relaxation) between the neighboring Er^{3+} ions strongly influence the intensity of the conversion and up-conversion PL. The investigation of the temperature dependence of PL indicates that erbium-doped chalcogenide semiconductors can be recommended as materials for the design of non-contact optical thermometers.

Author details


Volodymyr V. Halyan^{1*} and Inna A. Ivashchenko²

¹ Department of Experimental Physics and Technologies for Information Measuring, Lesya Ukrainka Eastern European University, Lutsk, Ukraine

² Department of Inorganic and Physical Chemistry, Lesya Ukrainka Eastern European University, Lutsk, Ukraine

*Address all correspondence to: halyan.volodimir@eenu.edu.ua

IntechOpen

© 2018 The Author(s). Licensee IntechOpen. This chapter is distributed under the terms of the Creative Commons Attribution License (<http://creativecommons.org/licenses/by/3.0>), which permits unrestricted use, distribution, and reproduction in any medium, provided the original work is properly cited. 

References

- [1] Frumar M, Wagner T. Ag doped chalcogenide glasses and their applications. *Current Opinion in Solid State and Materials Science*. 2003;7: 117-126. DOI: 10.1016/S1359-0286(03)00044-5
- [2] Kevshin A, Halyan V, Davydyuk G, Parasyuk O, Mazurets I. Concentration dependence of the optical properties of glassy alloys in the HgS-Ga₂S₃-GeS₂ system. *Glass Physics and Chemistry*. 2010;36:27-32. DOI: 10.1134/S1087659610010050
- [3] Yang G, Xia F, He X, Wen J, Chen G. Effects of Pb on thermal stability and crystallization kinetics of GeS₂-Sb₂S₃-PbS glasses. *International Journal of Applied Glass Science*. 2016;7:337-344. DOI: 10.1111/ijag.12181
- [4] Plotnichenko V, Philippovskiy D, Sokolov V, Sukhanov M, Velmuzhov A, Churbanov M, et al. Infrared luminescence in Bi-doped Ge-S and As-Ge-S chalcogenide glasses and fibers. *Optical Materials Express*. 2014;4:366-374. DOI: 10.1364/OME.4.000366
- [5] Bordovsky G, Marchenko A, Rabchanova T, Seregin P, Terukov E, Ali H. Study of platinum impurity atom state in vitreous arsenic selenide. *Semiconductors*. 2012;46:878-881. DOI: 10.1134/S1063782612070056
- [6] Marchenko A, Rabchanova T, Seregin P, Zharkoy A, Bobokhuzhaev K. Structural chemical states of dopant atoms of platinum and gold in glass-like arsenic selenides. *Glass Physics and Chemistry*. 2016;42: 43-49. DOI: 10.1134/S1087659616010077
- [7] Ivashchenko I, Danyliuk I, Olekseyuk I, Pankevych V, Halyan V. Phase equilibria in the quasi-ternary system Ag₂S-Ga₂S₃-In₂S₃ and optical properties of (Ga₅₅In₄₅)₂S₃₀₀, (Ga_{54.59}In_{44.66}Er_{0.75})₂S₃₀₀ single crystals. *Journal of Solid State Chemistry*. 2015;227:255-264. DOI: 10.1016/j.jssc.2015.04.006
- [8] Halyan V, Kevshyn A, Ivashchenko I, Shevchuk M. Effect of the substitution of S for Se on the optical absorption spectra of the glassy alloys Ag_{1.6}Ga_{1.6}Ge_{31.2}S_{61.6-x}Se_x. *Physics and Chemistry of Solid State*. 2016;17: 342-345. DOI: 10.15330/pcss.17.3.342-345
- [9] Mott N, Davis E. *Electronic Processes in Non-Crystalline Materials*. Oxford: Clarendon-Press; 1971. 437 p. DOI: 10.1002/crat.19720070420
- [10] Koughia K, Munzar M, Tonchev D, Haugen C, Decorby R, McMullin J, et al. Photoluminescence in Er-doped Ge-Ga-Se glasses. *Journal of Luminescence*. 2005;112:92-96. DOI: 10.1016/j.jlumin.2004.09.002
- [11] Halyan V, Kevshyn A, Kogut Y, Davydyuk G, Shevchuk M, Kažukauskas V, et al. Photoluminescence in Er-doped AgGaS₂-GeS₂ glasses. *Physica Status Solidi C*. 2009;6:2810-2813. DOI: 10.1002/pssc.200982576
- [12] Halyan V, Konchits A, Shanina B, Krasnovyd S, Lebed O, Kevshyn A, et al. EPR of γ -induced defects and their effects on the photoluminescence in the glasses of the Ag_{0.05}Ga_{0.05}Ge_{0.95}S₂-Er₂S₃ system. *Radiation Physics and Chemistry*. 2015;115:189-195. DOI: 10.1016/j.radphyschem.2015.06.019
- [13] Halyan V, Strelchuk V, Yuhymchuk V, Kevshyn A, Davydyuk G, Shevchuk M, et al. Role of structural ordering on optical properties of the glasses Ag_{0.05}Ga_{0.05}Ge_{0.95}S₂-Er₂S₃. *Physica B: Condensed Matter*. 2013;411: 35-39. DOI: 10.1016/j.physb.2012.10.042

- [14] Halyan V, Kevshyn A, Davydyuk G, Shevchuk M. Mechanism of anti-stokes photoluminescence in $\text{Ag}_{0.05}\text{Ga}_{0.05}\text{Ge}_{0.95}\text{S}_2\text{-Er}_2\text{S}_3$ glassy alloys. *Glass Physics and Chemistry*. 2013;**39**:52-56. DOI: 10.1134/S1087659613010069
- [15] Tver'yanovich Y. Concentration quenching of luminescence of rare-earth ions in chalcogenide glasses. *Glass Physics and Chemistry*. 2003;**29**: 166-168. DOI: 10.1023/A:1023407125519
- [16] Halyan V, Kevshyn A, Ivashchenko I, Olekseuk I, Danyliuk I, Shavarova G. Optical absorption of chalcogenide glass $\text{Ga}_2\text{S}_3\text{-La}_2\text{S}_3$ doped with erbium. *Physics and Chemistry of Solid State*. 2017;**18**: 342-346. DOI: 10.15330/pcss.18.3.342-346
- [17] Ivanova Z, Zavadil J, Rao K. Compositional trends in low-temperature photoluminescence of heavily Er-doped $\text{GeS}_2\text{-Ga}_2\text{S}_3$ glasses. *Journal of Non-Crystalline Solids*. 2011; **357**:2443-2446. DOI: 10.1016/j.jnoncrysol.2010.11.075
- [18] Kityk I, Halyan V, Yukhymchuk V, Strelchuk V, Ivashchenko I, Zhydashchuk Y, et al. NIR and visible luminescence features of erbium doped $\text{Ga}_2\text{S}_3\text{-La}_2\text{S}_3$ glasses. *Journal of Non-Crystalline Solids*. 2018;**498**:380-385. DOI: 10.1016/j.jnoncrysol.2018.03.024
- [19] Chen F, Jie W. Growth and photoluminescence properties of CdS solid solution semiconductor. *Crystal Research and Technology*. 2007;**42**: 1082-1086. DOI: 10.1002/crat.200710955
- [20] Era K, Shionoya S, Washizawa Y. Mechanism of broad-band luminescences in ZnS phosphors—I. Spectrum shift during decay and with excitation intensity. *Journal of Physics and Chemistry of Solids*. 1968;**29**: 1827-1841. DOI: 10.1016/0022-3697(68)90167-4
- [21] Kostka P, Zavadil J, Iovu M, Ivanova Z, Furniss D, Seddon A. Low-temperature photoluminescence in chalcogenide glasses doped with rare-earth ions. *Journal of Alloys and Compounds*. 2015;**648**:237-243. DOI: 10.1016/j.jallcom.2015.05.135
- [22] Khyzhun O, Halyan V, Danyliuk I, Ivashchenko I. Electronic structure of $(\text{Ga}_{55}\text{In}_{45})_2\text{S}_{300}$ and $(\text{Ga}_{54.59}\text{In}_{44.66}\text{Er}_{0.75})_2\text{S}_{300}$ single crystals. *Journal of Materials Science: Materials in Electronics*. 2016;**27**:3258-3264. DOI: 10.1007/s10854-015-4153-2
- [23] Kityk I, Yukhymchuk V, Fedorchuk A, Halyan V, Ivashchenko I, Oleksieyuk I, et al. Laser stimulated piezo-optics of γ -irradiated $(\text{Ga}_{55}\text{In}_{45})_2\text{S}_{300}$ and $(\text{Ga}_{54.59}\text{In}_{44.66}\text{Er}_{0.75})_2\text{S}_{300}$ single crystals. *Journal of Alloys and Compounds*. 2017;**722**:265-271. DOI: 10.1016/j.jallcom.2017.06.072
- [24] Halyan V, Khyzhun O, Ivashchenko I, Kevshyn A, Oleksieyuk I, Tyshchenko P, et al. Electronic structure and optical properties of $(\text{Ga}_{70}\text{La}_{30})_2\text{S}_{300}$ and $(\text{Ga}_{69.75}\text{La}_{29.75}\text{Er}_{0.5})_2\text{S}_{300}$ single crystals, novel light-converting materials. *Physica B: Condensed Matter*. 2018;**544**: 10-16. DOI: 10.1016/j.physb.2018.05.023
- [25] Ivashchenko I, Halyan V, Kevshyn A, Kubatska T, Rosolovska V, Tishchenko P, et al. Physical properties of the $(\text{Ga}_{70}\text{La}_{30})_2\text{S}_{300}$, $(\text{Ga}_{69.75}\text{La}_{29.75}\text{Er}_{0.5})_2\text{S}_{300}$ single crystals. *Acta Physica Polonica A*. 2018;**133**: 994-996. DOI: 10.12693/APhysPolA.133.994
- [26] Halyan V, Kityk I, Kevshyn A, Ivashchenko I, Lakshminarayana G, Shevchuk M, et al. Effect of temperature on the structure and luminescence properties of $\text{Ag}_{0.05}\text{Ga}_{0.05}\text{Ge}_{0.95}\text{S}_2\text{-Er}_2\text{S}_3$ glasses. *Journal of Luminescence*. 2017; **181**:315-320. DOI: 10.1016/j.jlumin.2016.09.022
- [27] Kuznetsov A, Velazquez J, Tikhomirov V, Mendez-Ramos J,

Moshchalkov V. Quantum yield of luminescence of Ag nanoclusters dispersed within transparent bulk glass vs. glass composition and temperature. *Applied Physics Letters*. 2012;**101**: 251106. DOI: 10.1063/1.4772957

[28] Agafonova D, Kolobkova E, Sidorov A. Temperature dependence of the luminescence intensity in optical fibers of oxyfluoride glass with CdS and $\text{CdS}_x\text{Se}_{1-x}$ quantum dots. *Technical Physics Letters*. 2013;**39**:629-631. DOI: 10.1134/S1063785013070158

IntechOpen